Philosophical Magazine

ISSN: 1478-6435 (Print) 1478-6443 (Online) Journal homepage: http://www.tandfonline.com/loi/tphm20

Ferromagnetism in amorphous MgO

Murat Durandurdu

To cite this article: Murat Durandurdu (2017) Ferromagnetism in amorphous MgO, Philosophical Magazine, 97:24, 2129-2141, DOI: 10.1080/14786435.2017.1328134

To link to this article: http://dx.doi.org/10.1080/14786435.2017.1328134

Published online: 10 May 2017.

PHILOSOPHICAL MAGAZINE, 2017
VOL. 97, NO. 24, 2129–2141
https://doi.org/10.1080/14786435.2017.1328134

Taylor & Francis
Taylor & Francis Group

Ferromagnetism in amorphous MgO

Murat Durandurdu

Department of Materials Science & Nanotechnology Engineering, Abdullah Gül University, Kayseri, Turkey

ABSTRACT

We report, for the first time, the atomic structure of amorphous MgO based on *ab initio* molecular dynamics simulations. We find that its main building blocks are four-fold and five-fold coordinated configurations, similar to those formed in the liquid state. Its average coordination is estimated to be about 4.36. The amorphous form having a perfect stoichiometry has a band gap energy of 2.4 eV. On the other hand, Mg vacancies induce an insulator to metal transition and ferromagnetism in amorphous MgO whilst O vacancies do not cause such a transition, implying that the magnetism in amorphous MgO is related to the non-stoichiometry and Mg vacancies. With the application of pressure, the stoichiometric and non-stoichiometric (Mg vacancies) models undergo a phase transformation into a rocksalt state, suggesting that the electronic structure of the initial configurations has no influence on the resulting high-pressure phase in amorphous MgO.

ARTICLE HISTORY
Received 9 June 2016
Accepted 1 May 2017

KEYWORDS
Ferromagnetism; Amorphous; MgO; Phase Transformation

1. Introduction

Magnesium oxide (MgO), or magnesia, is one of the extensively studied materials because of its importance in Materials Science and Geological Sciences. The significance of MgO in Materials Science is associated with its unique physical properties and important applications in technology and industry [1–4]. MgO is one of major components of planetary mantles and hence it has attracted considerable attentions in Geological Sciences as well. Considerable research efforts have been devoted to understand the thermodynamic properties of not only solid MgO but also liquid MgO under extreme high-pressure and temperature conditions [5–14] because such thermodynamic information can lead to the development of models for planets' interior.

The ground state of MgO is the six-fold coordinated rocksalt (RS) structure. At high pressure, the RS-to-CsCl phase transformation proposed in various theoretical investigations [15–18] was recently confirmed in a shock compression

CONTACT Murat Durandurdu murat.durandurdu@agu.edu.tr

experiment at 0.36 TPa [5]. In addition to the RS-to-CsCl phase change, a metallic liquid phase was predicted above 0.60 TPa in the same experiment [5]. Yet the information about this high-pressure metallic liquid state at the atomistic level is not clear yet, to our knowledge.

The liquid state of MgO at atmospheric pressure seems to have unusual electronic and structural properties, compared to the RS crystal [6]. Explicitly, its short-range order and electronic structure appear to be different from those of the crystalline counterpart: it has an average coordination number (CN) of 4.5–5 and presents a metallic character [6]. With the application of pressure, the liquid phase attained high coordinated configurations as expected and its mean CN was estimated to be more than seven at 150 GPa [6].

Recently amorphous form of MgO (*a*-MgO) was produced in several experiments [19–21]. The amorphous state has a poor MgO stoichiometry and exhibits the room temperature ferromagnetism. Non-stoichiometry and Mg vacancies were proposed to be responsible for this unusual magnetism [19–21]. First-principles simulations on the RS structure provided supportive evidence for this suggestion and further notified that Mg vacancies could drive an insulator-semimetal transition and ferromagnetism even in the crystalline MgO [22–25]. Additionally, some studies suggested that MgO could present magnetism when it was doped with both metallic and non-metallic elements as well [23–31].

It should be noted here that a disorder induced ferromagnetism can be reachable in some materials [32] and hence the distortion due to Mg vacancies or dopants might have some contribution to the ferromagnetism in MgO systems as well.

Since *a*-MgO shows a poor stoichiometry, *a*-MgO with exactly 1:1 stoichiometry might *currently* be considered as a hypostatical structure but modelling *a*-MgO can grant us to uncover whether there is any correlation between magnetism and disorder in MgO. Therefore, in the present work, we apply an *ab initio* molecular dynamics (MD) technique to generate an *a*-MgO model having perfect stoichiometry from its liquid state and non-stoichiometric *a*-MgO models by creating both Mg and O vacancies in the stoichiometry amorphous network. Amongst all these models, the ferromagnetism is observed for the one with Mg vacancies, proposing that the disorder nature of *a*-MgO has no influence on the magnetism. Under pressure, the crystallisation into a RS structure is witnessed for the stoichiometric and non-stoichiometric (Mg vacancies) models. This finding means that the electronic structure has no impact on the transformation mechanism in *a*-MgO.

2. Methodology

First principle MD calculations were performed by the SIESTA program [33] using norm-conserving Troullier–Martins pseudopotentials [34] and the generalised gradient approximation (Becke gradient exchange functional [35] and Lee, Yang and Parr correlation functional [36]). The calculations were carried out using the DZP orbitals. Γ point for the Brillouin zone integration was used

to generate an amorphous model having 1:1 stoichiometry. The MD simulations were performed within a canonical NPT ensemble. Temperature and pressure were controlled by the velocity rescaling and Parrinello–Rahman [37] methods. The initial rocksalt structure with 216 atoms was exposed to 5000 K for 4.0 ps. The applied temperature was then decreased to 3500 K within 2.0 ps. At 3500 K, the system was equilibrated for 20 ps. The liquid structure was then cooled to 1750 K in 15 ps, at which point the system remained disordered. An amorphous state was only achieved if the system was cooled to 300 K in about 10.0 ps. For the slower cooling rates (15–20 ps), on the other hand, the crystallisation into a RS structure was observed as shown in Figure 1. Finally, the configuration was optimised using the force tolerance of 0.01 eV/Å. In order to create non-stoichiometral models, one or two Mg or O atoms were removed from the network and then the systems were relaxed. For the non-stoichiometric *a*-MgO models, four special k points were used. In order to explore their high-pressure behaviour, we applied the constant pressure relation technique using the Parrinello–Rahman method.

3. Results

3.1. Atomic structure of liquid and amorphous MgO

The microstructure of the liquid (3500 K) and amorphous states can be probed and compared by numerous analysing techniques. The first technique that we consider here is partial pair distribution functions (PPDFs) that are frequently used to differentiate atomic bonding. The computed PPDFs are plotted in Figure 2. The Mg–O bond length is found to be 2.01 Å for the liquid state and 2.02 Å for the amorphous phase, suggesting that the first neighbour separation in the disordered MgO is not too sensitive to temperature. The Mg–O bond distance is, on the other hand, calculated to be 2.14 Å for the RS phase, comparable with the experimental result of 2.1 Å [38]. Since the Mg–O bond length correlates with CN and decreases with decreasing CN [39], its shortening in the amorphous and liquid states can be attributed to their average CN that is considerably less than

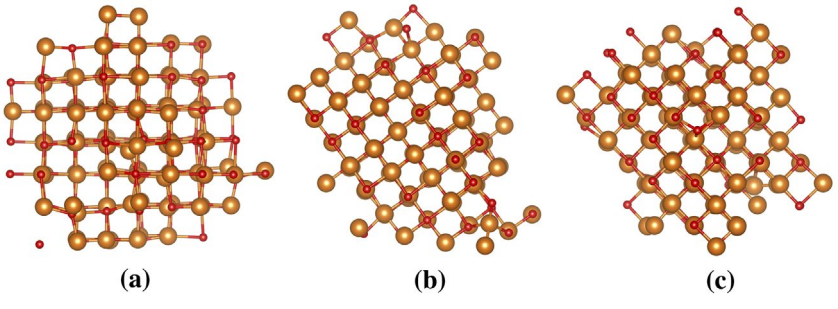

Figure 1. (colour online) The RS structure obtained (a) during the quenching from the liquid state (b) at 20 GPa for the stoichiometric *a*-MgO model and (c) at 20 GPa for the non-stoichiometric (two Mg vacancies) *a*-MgO model.

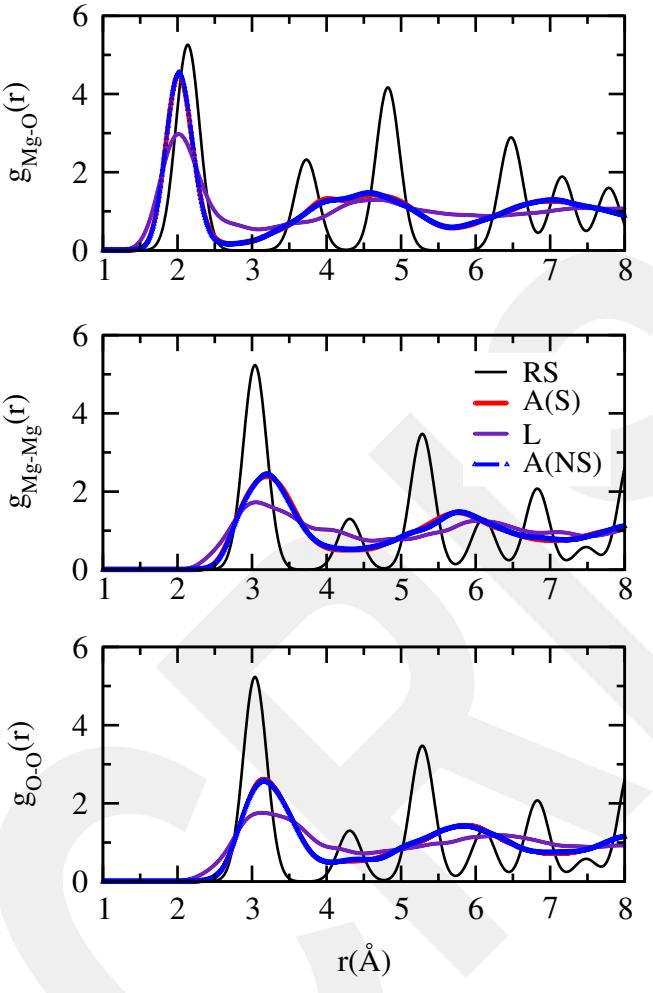

Figure 2. (colour online) Partial Pair distribution functions of the RS structure, the liquid MgO (L) the stoichiometric *a*-MgO model [A(S)] and the non-stoichiometric (two Mg vacancies) *a*-MgO model [A(NS)].

that of the RS phase as it will be discussed below. On the other hand, the Mg–Mg and O–O correlations of amorphous state are found to be longer than those of the RS phase. Inducing Mg vacancies does not result in a noticeable change in PPDFs. Such an effect might be expected because the concentration of vacancies created in the model is fairly small.

We next focus on the average CN, one of the most important structural quantities, which defines the atomic arrangements in materials. The average CN of the liquid and amorphous phases is estimated to be about 4.58 and 4.36, respectively. The predicted CN for the liquid state is in well agreement with the earlier first principles data of 4.5–5.0 [6]. Figure 3 illustrates the coordination distribution of Mg and O atoms. It seems that the main building units of the liquid and amorphous forms are the five-fold and four-fold configurations.

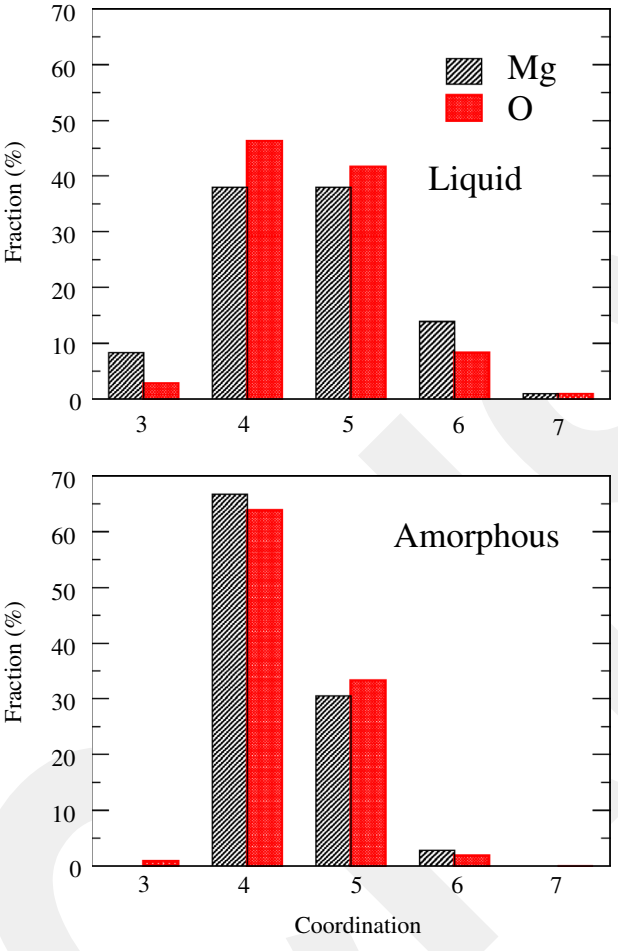

Figure 3. (colour online) Coordination distribution of Mg and O atoms for the liquid MgO and the stoichiometric *a*-MgO model.

Yet the amorphous state has more four-fold coordinated structures than the liquid state. Based on the number of the six-fold coordinated arrangements, one can see that the liquid state carries more characteristics of the RS-like structure than the amorphous form. The six-fold coordinated clusters are slightly deformed octahedrons whereas the five-fold coordinated ones have a pyramid shape with five atoms. Therefore, they are incomplete octahedrons. The absence of one atom at the base of the pyramid leads to a four-fold coordinated cluster. So they can be considered as an incomplete pyramidal configuration as well. As expected, the removal of Mg or O atoms in the model leads to a small decrease in the average CN to 4.28 (2 Mg vacancies) and 4.32 (two O vacancies).

Figure 4 shows the bond angle distributions functions. Disordered MgO systems exhibit very broad distributions. The angles range from 50° to 180° for the liquid state and from 65° to 180° for the amorphous one. Yet the main peak in

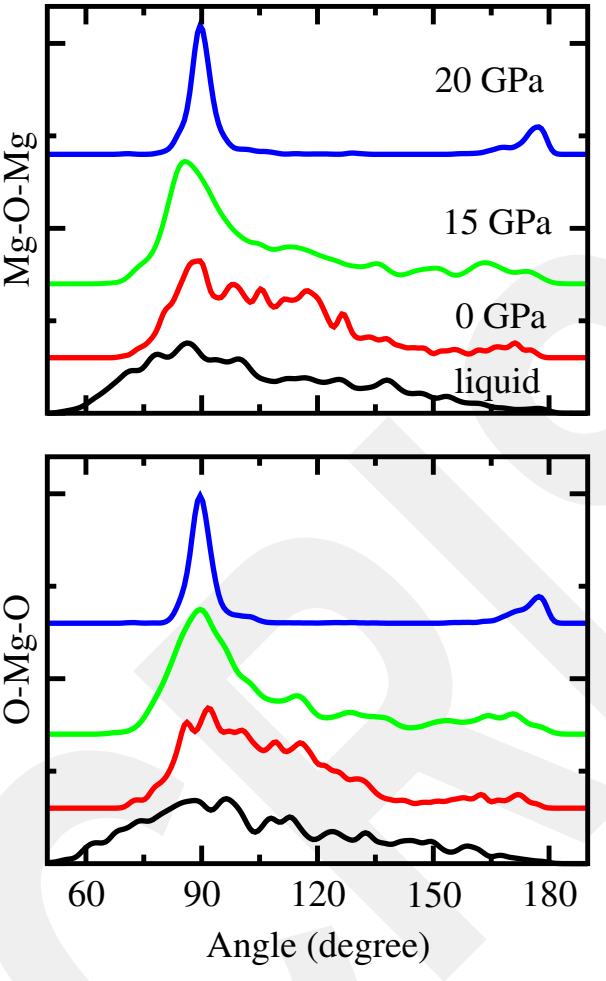

Figure 4. (colour online) Bond angle distribution functions of the liquid MgO and the stoichiometric *a*-MgO model at selected pressures.

all distributions is located around 90°, implying that the amorphous system has a trend to structure in octahedral-like units. As discussed above, the clusters observed in the models are closely related to each other hence it might be unsurprising to see a main peak near 90°.

3.2. Electronic structure

The electronic structure of the liquid, amorphous and RS phases of MgO is analysed by calculating the density of states (EDOS). The computed EDOSs are provided in Figure 5. The RS phase has a band gap energy of 4.2 eV that is, as anticipated, less than the experimental value of 7.8 eV because of the inadequacy of the DFT-GGA in describing exited states. The liquid state shows a semi-metallic character, according with the previous first-principle prediction [6]. On the other

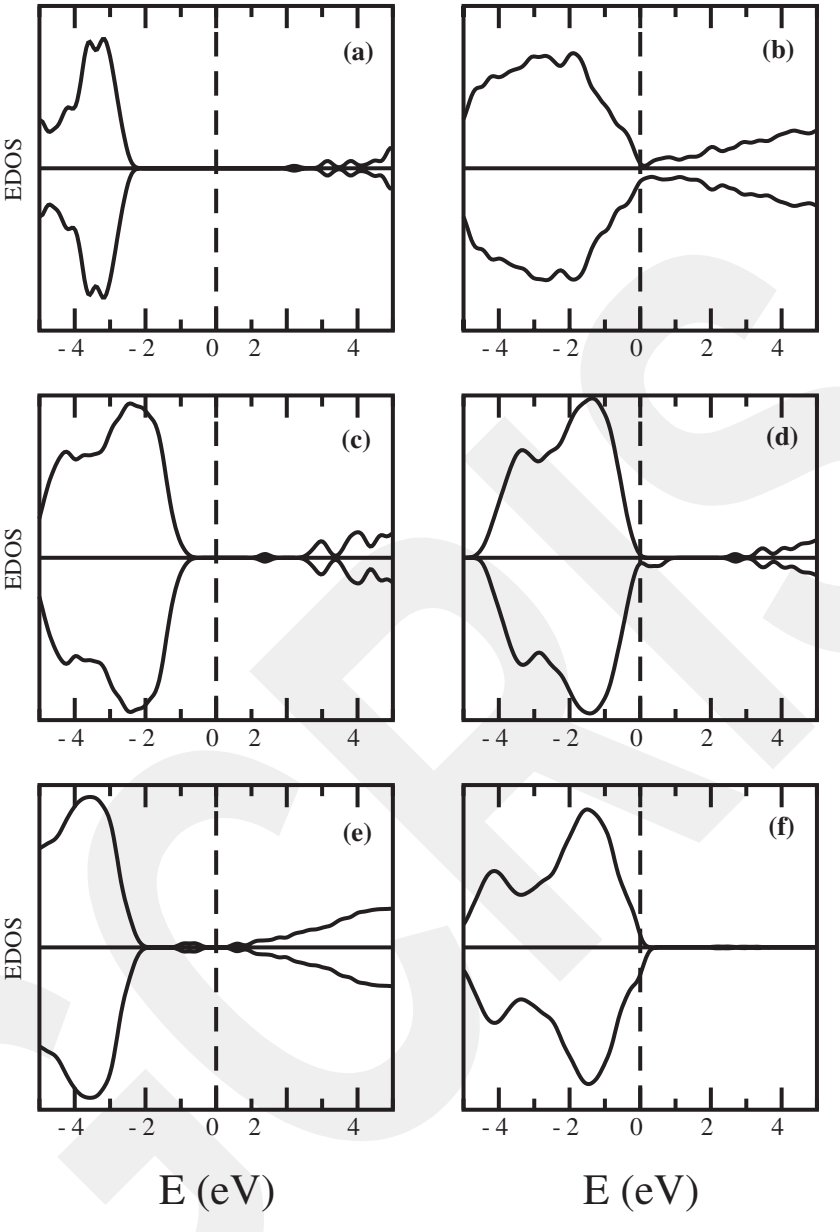

Figure 5. Electron density of states of (a) the RS structure, (b) the liquid MgO, (c) the stoichiometric *a*-MgO model (d) the non-stoichiometric (two Mg vacancies) *a*-MgO model, (e) the non-stoichiometric (two O vacancies) *a*-MgO model and (f) O-2p electrons for the non-stoichiometric (two Mg vacancies) *a*-MgO model. The dashed line is the Fermi Level.

hand, *a*-MgO has a clean band gap energy of about 2.3 eV. Neither the liquid state nor the amorphous state exhibits ferromagnetism because no spin polarisation is spotted for them. However, even a single Mg vacancy leads to spin splitting and an insulator to metal transition in *a*-MgO. This is mainly due to the spin polarisation of the O-2p electrons. The magnetic moment for *a*-MgO is estimated to be $1.99\mu_B$

and 3.99μ_B for the single and two Mg vacancies, respectively. O vacancies, on the other hand, do not produce such a transition although they yield midgap states below the Fermi level and a shift of the valence band to lower energies. We also investigate the influence of Mg vacancies on the crystalline RS phases and calculate its magnetic moment to be 1.95μ_B and 3.94μ_B for one and two Mg vacancies. These findings mean that the ferromagnetism in *a*-MgO is associated with Mg vacancies and non-stoichiometry, supporting to the earlier prediction and the disorder has almost no contribution to the magnetic moment.

The band gap energy of the RS phase is underestimated by a factor of ~1.85 in the simulation, relative to the experiment and hence *a*-MgO having a perfect 1:1 stoichiometry is expected to have a band gap energy of ~4.3 eV in experiment, signifying that *a*-MgO, if it is producible experimentally, can serve as a wide band gap semiconductor.

3.3. Pressure-induced phase transition in amorphous MgO

In order to understand the thermodynamic of the stoichiometric and non-stoichiometric (two Mg vacancies) models, we study their response to high-pressure. Such an investigation allows us to expose if their electronic structure has any impact on the transformation mechanism in *a*-MgO. We first consider the variation of volume provided in Figure 6 because the pressure volume relation can classify the thermodynamic nature of a phase transition. The models exhibit a different equation of state under pressure. The phase transformation occurs between 15 and 20 GPa in the stoichiometric model whilst it takes place between

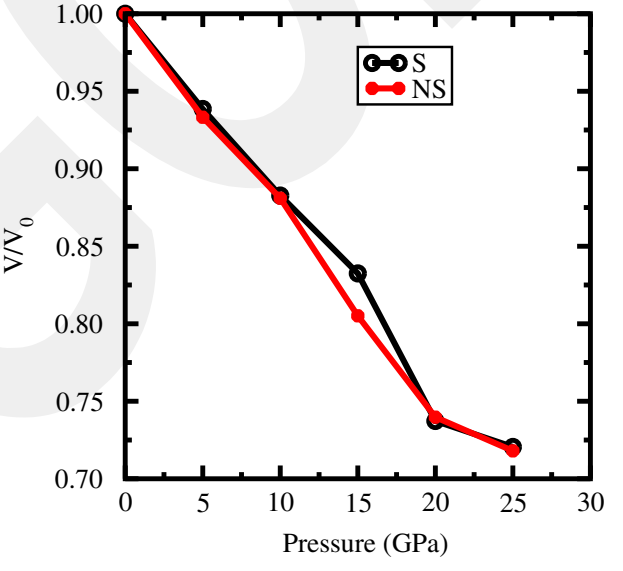

Figure 6. (colour online) Pressure–volume relation for the stoichiometric *a*-MgO model (S) and the non-stoichiometric (two Mg vacancies) *a*-MgO model (NS).

10 and 20 GPa in the defected one. The vacancies are expected to accelerate a phase transformation and hence the phase change started at a lower pressure in the defected (Mg vacancies) model.

Some information regarding the pressure-induced topological changes at the atomistic level can be obtained from PPDFs as shown in Figure 7. *a*-MgO still remains amorphous at 15 GPa for the stoichiometric and non-stoichiometric models. At 20 GPa, the appearance of sharp peaks at long-range order reveals

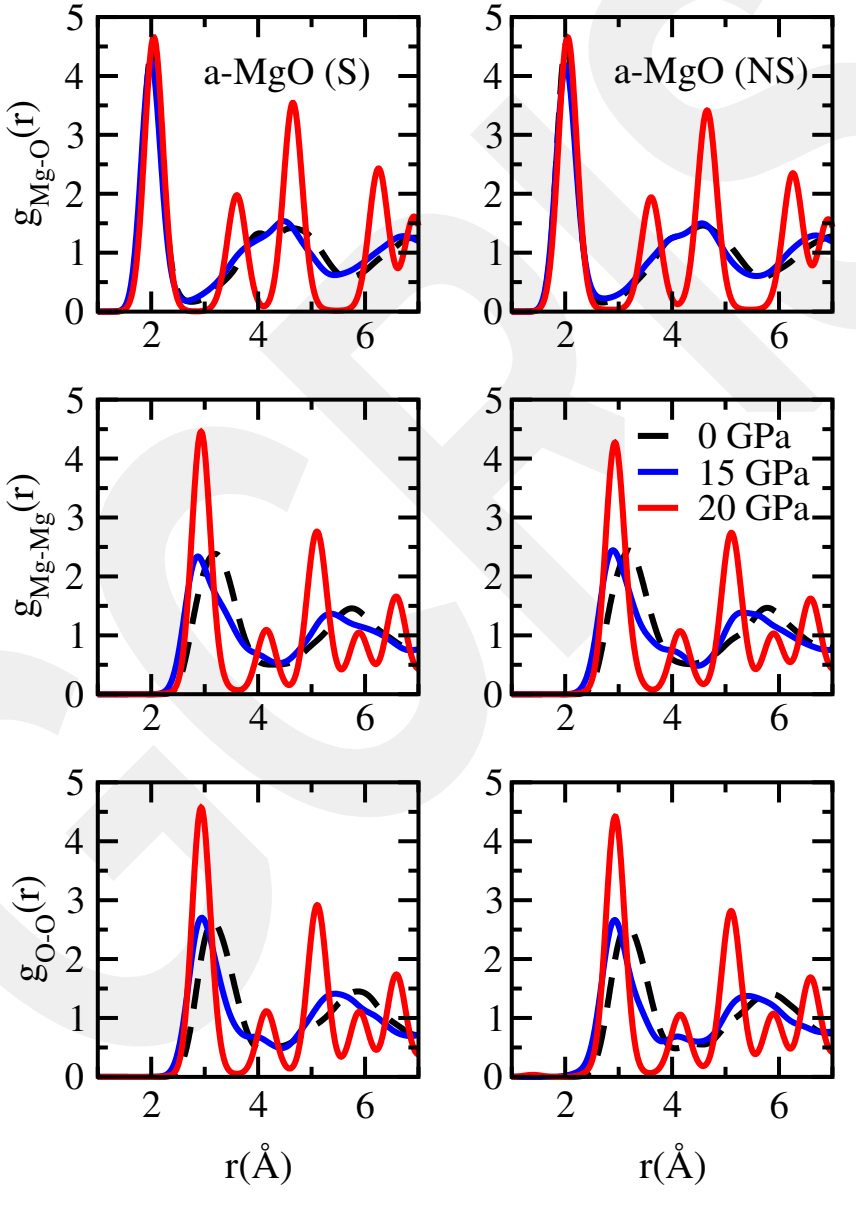

Figure 7. (colour online) Partial Pair distribution functions of the stoichiometric *a*-MgO model (S) and the non-stoichiometric (two Mg vacancies) *a*-MgO model (NS) at selected pressures.

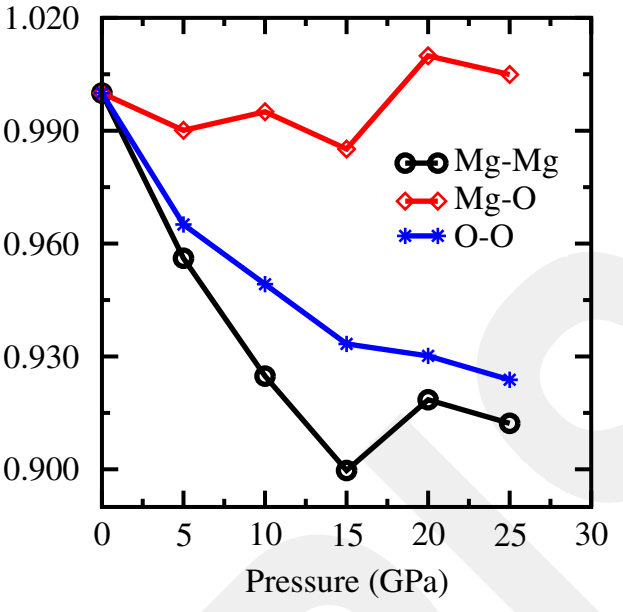

Figure 8. (colour online) Variation of Mg–O, Mg–Mg and O–O correlations (normalised) as a function of pressure for the stoichiometric *a*-MgO model.

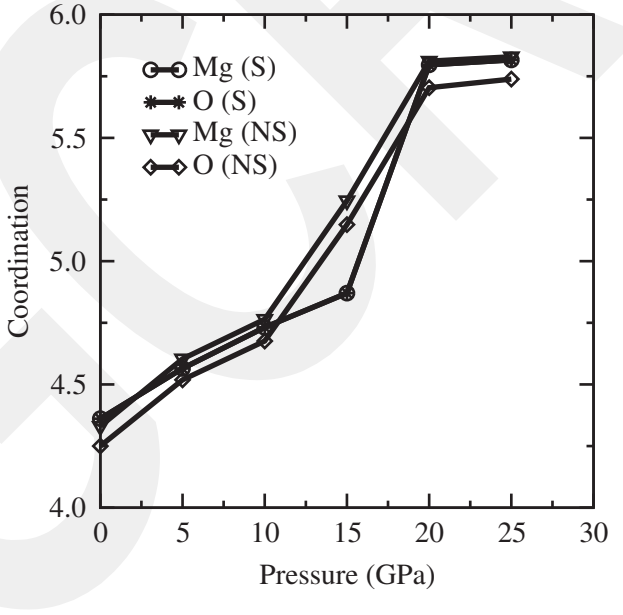

Figure 9. (colour online) Variation of Mg and O atoms as a function of pressure for the stoichiometric *a*-MgO model (S) and the non-stoichiometric (two Mg vacancies) *a*-MgO model (NS).

a pressure-induced crystallisation in *a*-MgO systems. As exposed in Figure 1, both networks transform into a RS structure that exhibits some structural defects. Figure 8 illustrates the influence of the external pressure on the atomic correlations.

Surprisingly, we find that pressure has an insignificant impact on the Mg–O bond distance (the change in Mg–O bonding under pressure is about 1%) even though the change in the average CN is severe whilst it noticeably reduces the O–O and Mg–Mg correlations. This finding is indeed different than our expectation because the rise in the average CN generally produces an increase in the first neighbour separation.

The pressure-induced structural rearrangements are well reflected in the BADFs as illustrated in Figure 4. With increasing pressure, the peak near 90° is sharpened and its intensity is increased gradually. A peak around 180° is somewhat pronounced. These observations can be interpreted as a tendency of the systems to form more octahedral-like configurations with the application of pressure.

Figure 9 presents the partial CNs as a function of pressure. For the stoichiometric and the non-stoichiometric amorphous networks, the average CNs increase slowly and owing to the crystallisation they suddenly jump to a value of ~6.

4. Conclusions

We have applied *ab initio* MD simulations to create an *a*-MgO model using the melt and quench technique. The short-range order of *a*-MgO is found to quite similar to that of the liquid state whose main building units are four-fold and five-fold coordinated incomplete octahedral-like configurations. The electronic structure calculations suggest that the liquid state is semimetal whereas the amorphous form having the ideal stoichiometry is a semiconductor with a band gap energy of 2.3 eV. The experimental band gap energy of *a*-MgO with a perfect stoichiometry is estimated to be about 4.3 eV and hence if *a*-MgO with a perfect stoichiometry is synthesized experimentally, it can serve as a wide gap semiconductor. The electronic structure calculations also indicate that introducing a small amount of Mg vacancies leads to ferromagnetism in the amorphous state. With the application of pressure, both magnetic and nonmagnetic *a*-MgO networks undergo a phase transformation into a RS structure.

Acknowledgement

The calculations were partially run on TÜBİTAK ULAKBİM, High Performance and Grid Computing Center (TRUBA resources).

Disclosure statement

No potential conflict of interest was reported by the author.

Funding

This work was supported by the Abdullah Gül University Support Foundation.

References

[1] S.S.P. Parkin, C. Kaiser, A. Panchula, P.M. Rice, B. Hughes, B. Smant, and S.H. Yang, *Giant tunnelling magnetoresistance at room temperature with MgO (100) tunnel barriers*, Nat. Mater. 3 (2004), pp. 862–867.

[2] M.V. Costache and J.S. Moodera, *All magnesium diboride Josephson junctions with MgO and native oxide barriers*, Appl. Phys. Lett. 96 (2010), pp. 082508–082510.

[3] R.H. Nibbelke, J. Scheerová, M.H.J.M. de Croon, and G.B. Maroon, *The oxidative coupling of methane over MgO-based catalysts: A steady-state isotope transient kinetic analysis*, J. Catal. 156 (1995), pp. 106–119.

[4] K. Sugiyama, K. Akazawa, M. Oshima, H. Miura, T. Matsuda, and O. Nomura, *Ammonia synthesis by means of plasma over MgO catalyst*, Plasma Chem. Plasma Process. 6 (1986), pp. 179–193.

[5] R.S. McWilliams, D.K. Spaulding, J.H. Eggert, P.M. Celliers, D.G. Hicks, R.F. Smith, G.W. Collins, and R. Jeanloz, Phase transformations and metallization of magnesium oxide at high pressure and temperature, Science 338 (2012), pp. 1330–1333.

[6] B.B. Karki, D. Bhattarai, and L. Stixrude, *First-principles calculations of the structural, dynamical, and electronic properties of liquid MgO*, Phys. Rev. B 73 (2006), pp. 174208–174214.

[7] A.B. Belonoshko, S. Arapan, R. Martonak, and A. Rosengren, *MgO phase diagram from first principles in a wide pressure-temperature range*, Phys. Rev. B 81 (2010), pp. 054110–054119.

[8] R.E. Cohen and Z. Gong, *Melting and melt structure of MgO at high pressures*, Phys. Rev. B 50 (1994), pp. 12301–12311.

[9] A. Aguado and P.A. Madden, New insights into the melting behavior of MgO from molecular dynamics simulations: The importance of premelting effects, Phys. Rev. Lett. 94 (2005), pp. 068501–068503.

[10] P. Tangney and S. Scandolo, *Melting slope of MgO from molecular dynamics and density functional theory*, J. Chem. Phys. 131 (2009), pp. 124510–124516.

[11] Z.J. Liu, X.W. Sun, Q.F. Chen, L.C. Cai, X.M. Tan, and X.D. Yang, *High pressure melting of MgO*, Phys. Lett. A 353 (2006), pp. 221–225.

[12] D. Alfè, Melting curve of MgO from first-principles simulations, Phys. Rev. Lett. 94 (2005), pp. 235701–235704.

[13] L. Vočadlo and G.D. Price, The melting of MgO – Computer calculations via molecular dynamics, Phys. Chem. Miner. 23 (1996), pp. 42–49.

[14] A. Zerr and R. Boehler, *Constraints on the melting temperature of the lower mantle from high-pressure experiments on MgO and magnesioüstite*, Nature 371 (1994), pp. 506–508.

[15] M.J. Mehl and R.E. Cohen, *RE and H. Krakauer, Linearized augmented plane wave electronic structure calculations for MgO and CaO*, J. Geophys. Res. 93 (1988), pp. 8009–8022.

[16] A.R. Oganov, M.J. Gillan, and G.D. Price, *Ab initio lattice dynamics and structural stability of MgO*, J. Chem. Phys. 118 (2003), pp. 10174–10182.

[17] J.E. Jaffe, J.A. Snyder, Z. Lin, and A.C. Hess, *LDA and GGA calculations for high-pressure phase transitions in ZnO and MgO*, Phys. Rev. B 62 (2000), pp. 1660–1665.

[18] B.B. Karki, L. Stixrude, S.J. Clark, M.C. Warren, G.J. Ackland, and J. Crain, *Structure and elasticity of MgO at high pressure*, Am. Mineral. 82 (1997), pp. 51–60.

[19] S.K. Mahadeva, J. Fan, A. Biswas, K.S. Sreelatha, L. Belova, and K.V. Rao, *Magnetism of amorphous and nano-crystallized Dc-sputter-deposited MgO thin films*, Nanomaterials 3 (2013), pp. 486–497.

[20] V. Harnchana, A.T. Hindmarch, A.P. Brown, R.M. Brydson, and C.H. Marrows, *TEM investigation of MgO thin films for magnetic tunnel junction application*, J. Phys. Conf. Ser. 241 (2010), pp. 012039–0120342.

[21] J. Li, Y. Jiang, G. Bai, T. Ma, D. Yang, Y. Du, and M. Yan, *Room temperature ferromagnetism of amorphous MgO films prepared by pulsed laser deposition*, Appl. Phys. A 115 (2014), pp. 997–1001.
[22] C. Martínez-Boubeta, J.I. Beltrán, L. Balcells, Z. Konstantinović, S. Valencia, D. Schmitz, J. Arbiol, S. Estrade, J. Cornil, and B. Martínez, *Ferromagnetism in transparent thin films of MgO*, Phys. Rev. B 82 (2010), pp. 024405–024411.
[23] F. Gao, J. Hu, C. Yang, Y. Zheng, H. Qin, L. Sun, X. Kong, and M. Jiang, *First-principles study of magnetism driven by intrinsic defects in MgO*, Solid State Commun. 149 (2009), pp. 855–858.
[24] B. Merabet, S. Kacimi, A. Mir, M. Azzouz, and A. Zaoui, *Vacancy effects on the electronic structure of MgO compound*, Mod. Phys. Lett. B 29 (2015), pp. 1550147–1550157.
[25] J.I. Beltrán, C. Monty, L. Balcells, and C. Martínez-Boubeta, *Possible d0 ferromagnetism in MgO*, Solid State Commun. 149 (2009), pp. 654–1657.
[26] K. Kenmochi, Van Ann Dinh, K. Sato, A. Yanase, and H. Katayama-Yoshida, *Materials design of transparent and half-metallic ferromagnets of MgO, SrO and BaO without magnetic elements*, J. Phys. Soc. Japan 73 (2004), pp. 2952–2954.
[27] M.M. Ibrahim, Z. Feng, J.C. Dean, and M.S. Seehra, *Magnetic susceptibilities of Co-and Ni-doped MgO*, J. Phys. Condens. Matter 4 (1992), pp. 7127–7134.
[28] C. Århammar, C. Moyses Araujo, K. Venkat Rao, S. Norgren, B. Johansson, and R. Ahuja, *Energetics and magnetic properties of V-doped MgO bulk and (001) surface: A GGA, GGA+ U, and hybrid density functional study*, Phys. Rev. B 82 (2010), pp. 134406–134414.
[29] V. Sharma, G. Pilania, and J.E. Lowther, *Ferromagnetism in IV main group element (C) and transition metal (Mn) doped MgO: A density functional perspective*, AIP Adv. 1 (2011), pp. 032129–032140.
[30] G. Liu, S. Ji, L. Yin, G. Fei, and C. Ye, *An investigation of the electronic properties of MgO doped with group III, IV, and V elements: Trends with varying dopant atomic number*, J. Phys. Condens. Matter 22 (2010), pp. 046002–046007.
[31] A. Droghetti and S. Sanvito, *Electron doping and magnetic moment formation in N-and C-doped MgO*, Appl. Phys. Lett. 94 (2009), pp. 252505–252507.
[32] C.M. Araujo, S. Nagar, M. Ramzan, R. Shukla, O.D. Jayakumar, A.K. Tyagi, Y.-S. Liu, J.L. Chen, P.A. Glans, C. Chang, A. Blomqvist, R. Lizárraga, E. Holmström, L. Belova, J. Guo, R. Ahuja, and K.V. Rao, *Disorder-induced Room Temperature Ferromagnetism in Glassy Chromites*, Scientific Reports 4 (2014).
[33] P. Ordejón, E. Artacho, and J.M. Soler, *Self-consistent order-N density-functional calculations for very large systems*, Phys. Rev. B 53 (1996), pp. R10441–R10444.
[34] N. Troullier and J.M. Martins, *Efficient pseudopotentials for plane-wave calculations*, Phys. Rev. B 43 (1991), pp. 1993–2006.
[35] A.D. Becke, *Density-functional exchange energy approximation with correct asymptotic behavior*, Phys. Rev. A 38 (1988), pp. 3098–3100.
[36] C. Lee, W. Yang, and R.G. Parr, *Development of the collesalvetti correlation-energy formula into a functional of the electron density*, Phys. Rev. B 37 (1988), pp. 785–789.
[37] M. Parrinello and A. Rahman, *Polymorphic transitions in single crystals: A new molecular dynamics method*, J. Appl. Phys. 52 (1981), pp. 7182–7190.
[38] I.F. Mironyuk, V.M. Gunko, M.O. Povazhnyak, V.I. Zarko, V.M. Chelyadin, R. Leboda, J. Skubiszewska-Zięba, and W. Janusz, *Magnesia formed on calcination of Mg (OH)2 prepared from natural bischofite*, Appl. Surf. Sci. 252 (2006), pp. 4071–4082.
[39] G.S. Rohrer, *Structure and Bonding in Crystalline Materials*, Cambridge University Press, Cambridge, 2011.